Transition metal promoted K/Mo2C as efficient catalysts for CO hydrogenation to higher alcohols

Journal:	*Catalysis Science & Technology*
Manuscript ID:	CY-ART-07-2015-001173.R1
Article Type:	Paper
Date Submitted by the Author:	25-Aug-2015
Complete List of Authors:	Liakakou, Eleni; Aristotle University of Thessaloniki, Chemical Engineering; Centre for Research and Technology Hellas, Chemical Process & Energy Resources Institute Heracleous, Eleni; Centre for Research and Technology Hellas, Chemical Process & Energy Resources Institute; International Hellenic University, School of Science & Technology

Catalysis Science & Technology

ARTICLE

Transition metal promoted K/Mo_2C as efficient catalysts for CO hydrogenation to higher alcohols

Received 00th January 20xx,
Accepted 00th January 20xx

DOI: 10.1039/x0xx00000x

www.rsc.org/

E.T. Liakakou[a, b] and E. Heracleous[a, c, *]

This study investigates the effect of transition metal promotion in a series of K/Mo_2C catalysts doped with Ni, Cu and Mn for the hydrogenation of CO to higher alcohols. The catalysts were found to produce a significant amount of higher alcohols, consisting mainly of linear alcohols with two to four carbon atoms, at mild reaction conditions (temperature of 280°C and pressure of 40-60 bar). All transition metals increased selectivity to higher alcohols compared to the reference material. Nickel had the most favorable effect, as it greatly increased CO conversion as well. XPS results revealed a strong interaction between molybdenum in the carbidic phase and the transition metals, indicative of electron transfer from the dopants to the Mo atoms. In the Ni/K/Mo_2C catalyst, the formation of a mixed Ni-Mo carbidic phase phase was evidenced. We postulate that this phase serves as the active center for non-dissociative CO chemisorption and leads, in combination with dissociative CO adsorption on the Mo_2C sites, to higher alcohol formation. Overall, the Ni/K/Mo_2C catalyst exhibited the highest catalytic activity, with a 23% CO conversion, 30.5% higher alcohol selectivity and space time yield to oxygenates of 147.4 mg/$g_{catalyst}$/h at 280°C and 60bar. Stability testing of the optimum catalyst for 400 hours time on stream demonstrated considerable deactivation, with an activity decrease of ~48%. The reduction in reactivity can be ascribed to the segregation of the mixed Ni-Mo carbidic phase and the formation of hydrated oxidic nickel species together with a well-defined $K_2Mo_2O_7$ phase.

Introduction

Research on alternative energy has become more important in recent years due to the continued depletion of conventional energy resources and the increased concentration of CO_2 in the atmosphere, leading to over-warming of the earth. The synthesis of higher alcohols from biomass-derived syngas (CO and H_2) is a potential approach to the production of "green" aviation fuels[1] and/or renewable chemicals and petrochemical feedstocks. The hydrogenation of carbon monoxide to the desired oxygenates takes place thermochemically at high pressures and intermediate temperatures[2] in the presence of a catalyst able to selectively activate CO and H_2 towards the synthesis of oxygenated molecules.

Several catalytic systems have been investigated for higher alcohol synthesis, such as modified low and high temperature Cu-based methanol synthesis catalysts, modified Co and Fe Fischer-Tropsch catalysts and Mo-based materials in oxidic and sulfided form[3-5]. Interest in the latter category commenced in the 1980s when researchers from Dow Chemical and Union Carbide reported the ability of alkali promoted MoS_2 to produce C_1-C_5 alcohols from syngas.[2] However, the detection of significant amounts of sulfur in the product renders this catalytic system problematic, especially for fuel product applications with strict sulfur specifications.

Molybdenum in its carbide form represents an interesting alternative. Mo_2C exhibits catalytic properties similar to those of noble metals and has been used as a cheaper substitute for noble metal catalysts in various reactions, such as CO hydrogenation to hydrocarbons and mixed alcohols,[6, 7] CO methanation,[8-10] hydrodenitrogenation (HDN),[11] hydrodesulfurization (HDS),[11] hydrocarbon isomerization,[12] etc. Various studies have shown that molybdenum carbides produce primarily light alkanes at atmospheric pressure.[9,13] The addition of alkalis is crucial in shifting the hydrogenation products from hydrocarbons to alcohols. Woo et al.[7] reported the first systematic investigation of alkali promoted molybdenum carbides for alcohol synthesis from syngas. In particular, promotion of molybdenum carbide with K_2CO_3 was found to greatly enhance selectivity to linear C_1–C_7 alcohols.[7, 14-17] Lee et al.[18] studied the promotional effect of several potassium salts (K_2CO_3, K_2SO_4 and KCl) on Mo_2C catalysts and suggested that the type of potassium salt affects the distribution of the promoters on the carbide surface, which in turn greatly influences the nature of the promotional effects in CO hydrogenation to alcohols. K_2CO_3 was found to form complexes with the carbide, well-distributed on the surface,

[a] Chemical Process & Energy Resources Institute (CPERI), Centre for Research and Technology Hellas (CERTH), 6th km Charilaou - Thermi Road, P.O. Box 361, 57001 Thessaloniki, Greece.
[b] Department of Chemical Engineering, Aristotle University of Thessaloniki, P.O.Box 1517, University Campus, 54124 Thessaloniki, Greece
[c] School of Science & Technology, International Hellenic University (IHU), 14th km Thessaloniki – Moudania, 57001 Thessaloniki, Greece
* email: eheracle@cperi.certh.gr

that promote molecular adsorption of CO and at the same time physically block sites that catalyze the hydrogenation of intermediates to hydrocarbons, exerting thus a geometric effect that increases alcohol formation. On the other hand, K_2SO_4 and KCl caused only slight increase in olefin selectivity with negligible alcohol formation. These promoters maintained their initial states and showed non-uniform distribution on the surface, mostly affecting the electron state of Mo_2C via an electronic effect. Muramatsu et al.[19] also studied the role of K promoter on Mo oxide for the same reaction and concluded that K inhibits both dehydration of alcohols to alkenes and hydrogenation of alkenes to alkanes.

Doping with transition metals has also been found to be beneficial for the synthesis of higher alcohols. The addition of transition metals (such as Co, Ni, Rh and Pd) has been reported to improve catalytic activity and selectivity to C_{2+} alcohols over MoS_2-based catalysts.[20-22] In a series of K-promoted oxidic Mo catalysts supported on activated carbon, we found that the Ni-Mo synergistic effect is essential for the activation of CO, as monometallic AC-supported Mo and Ni demonstrated complete inactivity toward CO hydrogenation.[23] The promotional effect of transition metals on Mo_2C-based catalysts for higher alcohol synthesis has been less studied. According to a review by Zaman and Smith,[24] the alcohol product distribution obtained over transition metal promoted K-M-Mo_2C catalysts (M = Fe, Co, or Ni) typically includes C_1-C_6 alcohols and hydrocarbons, both following the Anderson-Schulz-Flory (ASF) distribution. Comparing the probability of chain growth parameter for both hydrocarbons and alcohols, it was found that the addition of Fe, Co or Ni to the Mo_2C catalyst significantly increases the alcohol chain growth probability; however the chain growth probability for hydrocarbons was higher in all cases. The complexity of the promoted Mo_2C catalysts makes it difficult to unravel the role of each of the catalyst components in catalyst activity and selectivity. Nonetheless it is clear that increased concentration of the Group VIII metal results in increased higher alcohols production.[24]

Zhao et al.[25] reported that over Ni–Mo bimetallic carbide catalysts CO conversion monotonically increased with increasing Ni content. However, the space time yield of the alcohol products increased with increasing Ni content up to Ni/Mo ratio of 0.5, and then decreased with further increasing Ni content. Sun and co-workers[14] also studied K-Mo_2C promotion with Ni and suggested that the active phase for alcohol synthesis is a “K-Mo-C” phase which is enhanced by Ni dispersed within the Mo_2C. Aggregated Ni was argued to be responsible for hydrocarbon synthesis and alcohol chain propagation. The metal promoter also reduced the amorphous C that was present on the surface as a consequence of the Mo_2C synthesis. Similar conclusion were also drawn by the same group, regarding La and Ni co-modified K_2CO_3/MoS_2 catalysts.[26]

Copper and manganese also appear to be promising promoters in higher alcohol synthesis. It has been argued that methanol is the precursor in higher alcohols production and since Cu is a metal known for its activity in methanol synthesis, it is expected to increase the rate of CO hydrogenation to methanol, therefore accelerating the formation rate of higher alcohols.[27] Cu addition in Mo_2C led to lower hydrocarbon selectivity in CO_2 hydrogenation.[28] The use of Mn as promoter has also been reported to benefit the alcohol synthesis over a wide variety of catalytic systems.[29, 30] In one of our previous studies[31] the substitution of Zn by Mn in a series of K-Cu/Zn/Al catalysts was found to increase higher alcohol formation by 50%. This selectivity enhancement was ascribed to the reduced acidity of the K-Cu/Mn/Al catalyst which promoted aldol condensation reactions to higher alcohols.

Although several literature studies report the promotion of molybdenum carbide with transition metals for higher alcohol synthesis, it is still unclear how the promoters interact structurally with the carbide and how they affect the critical properties of the catalyst towards oxygenate formation. In this work, we investigate in a systematic manner the promotional effect of Ni, Cu and Mn in K/Mo_2C for the hydrogenation of carbon monoxide to higher alcohols. The study is focused on the structural and physiochemical properties of the catalysts and the alteration of these properties by the presence of the specific dopants in relation to the effect on the activity and selectivity to higher alcohols. Characterization results are thus combined with catalyst evaluation data in CO hydrogenation in an attempt to identify the functionalities of the transition metal promoted K/Mo_2C catalysts and the nature of the active sites.

Results and discussion

Catalyst characterization

The main physicochemical characteristics of the M-promoted K/Mo_2C (M = Ni, Mn, Cu) catalysts with a molar composition of $M_{0.25}K_{0.6}Mo_2C$ are tabulated in Table 1. The BET measurements show similar surface areas for the reference and the Ni- and Mn-promoted catalysts, in the range of 13-15 m^2/g. Increased surface area was recorded for the Cu/K/Mo_2C sample (21.8 m^2/g), however in general the addition of the metal promoters does not seem to significantly affect the textural properties of the materials. Overall, the surface areas of the catalysts are rather low, probably due to the high carburization temperature (up to 750 °C) and the high loading of K_2CO_3.[7] Wu[32] observed that the carburization process yields a bulk carbide with low surface area (11.5 m^2/g), however much larger than that of its oxidic precursor (3 m^2/g) due to the generation of pores during the carburization process. After the loading of K_2CO_3 (10 wt%), the surface area decreased significantly to 2.4 m^2/g indicating that K_2CO_3 blocks most of the pores created during carburization.

Table 1. Physicochemical characteristics of transition metal promoted M/K/Mo_2C catalysts, where M=Ni, Cu, Mn

Catalysts	K_2CO_3 loading, wt%	Transition metal loading, wt%	Surface area, m^2/g	Desorbed CO, mmol/g		Desorbed CH_4, mmol/g		H_2 consumption, mmol/g
				TPD	TPR	TPD	TPR	
K/Mo_2C	12.6	-	13.6	0.9	1.1	0.03	0.17	3.2
Ni/K/Mo_2C	8.9	6.1	15.6	1.4	1.8	0.02	0.15	3.0
Cu/K/Mo_2C	9.2	6.5	21.8	1.1	1.8	0.05	0.11	1.8
Mn/K/Mo_2C	9.1	5.7	13.3	0.8	1.4	0.05	0.06	1.0

X-ray Diffraction (XRD) was employed for identifying the crystalline phases in the investigated catalysts. The diffractograms shown in Fig. 1 evidence that all catalysts exhibit diffraction lines corresponding to a well-defined β-Mo_2C crystal phase (2θ = 34.4°, 38.0°, 39.4°, 52.1°, 61.5°, 69.6°, 74.6°, and 75.6°).[14] None of the samples displayed any MoO_2 diffractions, indicating successful carburization of the $MMoO_x$ precursors. Traces of K_2MoO_4 were detected in all catalytic materials, except from the Mn-promoted carbide where the MnO_2 crystal phase was identified. Additionally, a peak at 43.3° detected in Cu/K/Mo_2C was attributed to metallic Cu. In the Ni/K/Mo_2C catalyst, a small peak appearing at ~44° could be attributed to either metallic nickel or a mixed Ni-Mo carbide phase (Ni_6Mo_6C) which usually forms during the temperature-programmed carburization process.[33,34] The structure of Ni_6Mo_6C was analyzed by Newsam et al.[35] who claimed that the amorphous Ni–Mo carbide transformed into Ni_6Mo_6C crystallites upon heating at high temperature.

It is known that Mo_2C can incorporate large amounts of oxygen when exposed to air at room temperature.[36] Since oxygen is a poison for several reactions, it must be removed from the surface to activate the catalyst. Temperature programmed studies were performed in order to study the effect of transition metals on oxygen incorporation and ease of removal from the catalyst. Temperature programmed desorption in helium (TPD-He) was first performed to determine the oxygen removal properties and nature of desorbed species in inert atmosphere. Fig. 2 illustrates the CO, CH_4 and H_2O desorption profiles of all molybdenum carbide catalysts. An important finding is that oxygen is not removed from the samples as molecular O_2. Instead, it combines with bulk carbon in the sample and desorbs mainly as CO along with small amounts of CO_2. Quantitative results in terms of carbon monoxide and methane for the TPD-He experiments are shown in Table 1.

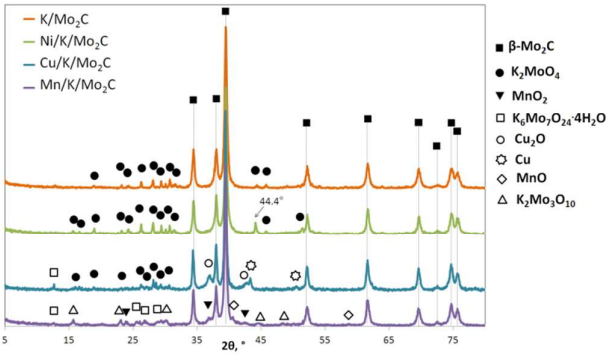

Figure 1. X-ray diffraction patterns of the transition metal promoted M/K/Mo2C catalysts, where M=Ni, Cu, Mn

The quantification of the amount of desorbed CO showed similar values, ranging from 0.8-1.1 mmol CO/g for the reference catalyst and the Cu and Mn-promoted carbides, which corresponds to loss of the catalyst carbon in the range of 20-30%. Relatively higher amount was calculated for the Ni-promoted K/Mo_2C, which could imply that the presence of nickel enhances oxygen incorporation in the material.[37] Water and small methane desorption peaks (Fig. 2) at 100°C and 700°C, respectively, were also observed. Desorption of water occurred at low temperature and is characteristic of the removal of physisorbed water from the samples. Methane was desorbed at high temperatures, but in negligible amounts, in the range of 0.02-0.05 mmol CH_4/g for all carbidic catalysts. The formation of methane may be attributed to reaction of carbon with either residual hydrogen that might have dissolved in the sample during synthesis, or with hydrogen produced from the dissociation of water strongly bound to the surface and/or water trapped in the pores of the catalyst.[36].
Concerning the profiles of CO evolution, all carbides exhibit large CO desorption from 620 – 800°C. The reference K/Mo_2C catalyst exhibits a big sharp desorption of CO around 700°C, consistent with the results of Bej et al.,[38] accompanied by a smaller peak at 760-775°C. The introduction of the promoters modified the evolution profile of CO from the carbide. Cu and Mn promoted K/Mo_2C catalysts show similar profiles with two desorption peaks, a sharp one at 695°C and a broader peak at ~760°C.[36] The sharp peak has similar characteristics with that of the reference material, shifted to lower temperature. The CO profile is however significantly different for the Ni promoted K/Mo_2C catalyst. There is a large broad desorption peak at high temperature (770°C), similar to that observed in the other promoted catalysts, however CO desorption starts earlier evidenced by an additional wide desorption peak at lower temperature (650°C).

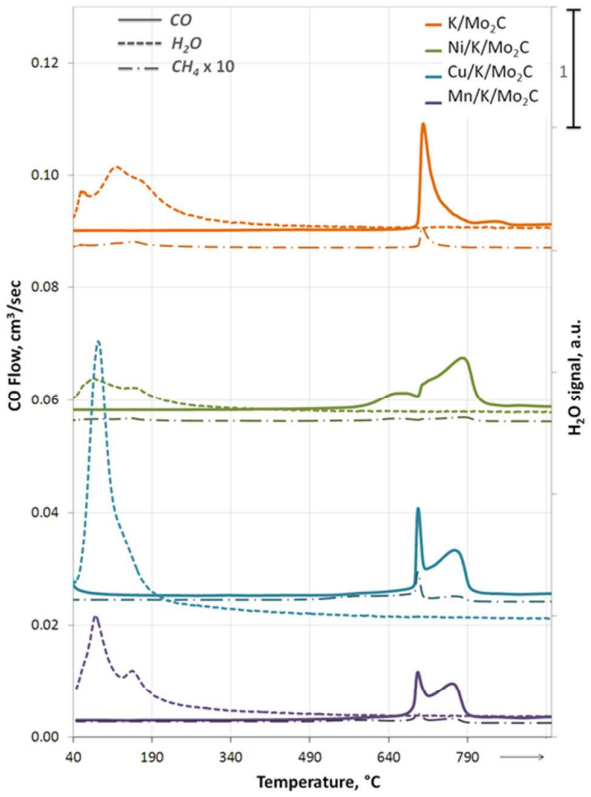

Figure 2. Temperature-programmed desorption profiles in He (TPD-He) of the transition metal promoted $M/K/Mo_2C$ catalysts, where M=Ni, Cu, Mn

The removal of oxygen from the catalysts in reductive atmosphere as well as the reducibility of the materials was studied by temperature programmed reduction in hydrogen ($TPR-H_2$). Figure 3 presents the H_2 consumption profiles and the CO, CH_4 and H_2O desorption profiles of the transition metal promoted K/Mo_2C catalysts. Small CO_2 desorption peaks were also observed during TPR (not shown). Quantitative results for the amount of hydrogen consumed as well as carbon monoxide and methane desorbed are given in Table 1. Concerning hydrogen consumption, the reference K/Mo_2C catalyst, as well as the Ni and Cu-promoted catalysts, exhibit similar reduction profiles with two reduction peaks, in the 300-375°C and the 550-690°C range. The Mn-promoted carbide demonstrates very low H_2 consumption, with only one wide reduction peak extending from 300 to 600°C, with a maximum at the temperature of 400°C. The consumption of hydrogen, accompanied by simultaneous water desorption, could originate both from the reaction of the oxygen incorporated in the carbides and also from the reduction of any oxidic phases which form on the catalyst surface during the passivation process. In comparison with the TPD-He experiments, it can be deduced that in the presence of hydrogen oxygen is removed at much lower temperatures than in inert atmosphere. Although almost half of the oxygen is removed as water (~50%), the rest still reacts with the carbon of the material and desorbs as CO. As shown in Fig. 3, all carbides exhibit large CO desorption from 620 – 850°C, presenting similar desorption profiles to the TPD-He (Fig. 2). Quantification of this CO shows that its quantity is in the same range or even higher to that removed under helium (Table 1). This indicates that at least part of the oxygen that is removed by hydrogen is incorporated oxygen and/or oxygen in formed oxides that exists in the materials and cannot be removed in inert atmosphere even at the high temperatures of 800°C. The total amount of oxygen removed from the carbides (both in water and CO) in hydrogen atmosphere follows the order of the TPD-He experiments, with the $Ni/K/Mo_2C$ exhibiting the highest oxygen removal. This enforces the notion that the presence of nickel enhances oxygen incorporation in the material.

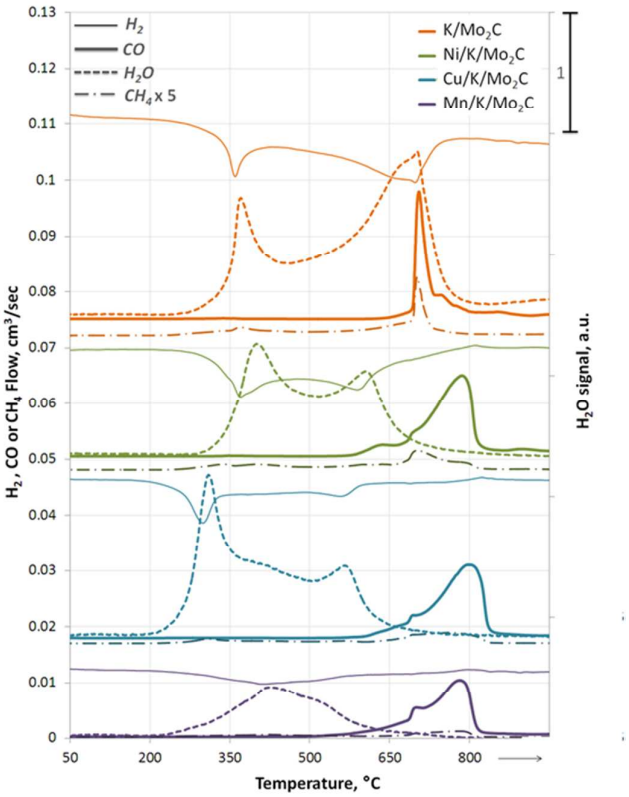

Figure 3. Temperature-programmed reduction profiles ($TPR-H_2$) of the transition metal promoted $M/K/Mo_2C$ catalysts, where M=Ni, Cu, Mn

Surprisingly, the amount of carbon that reacts with hydrogen to form methane is much lower than the reaction of carbon with oxygen. The amount of desorbed methane is of course higher in the presence of hydrogen than in helium (TPD-He experiments), but it is remains an order of magnitude lower than desorbed CO. The CH_4 desorption peaks appear in the 700-800°C range. At these temperatures, it is likely that methane is formed from the reaction of hydrogen with the carbidic carbon of the catalysts.[39] Methane originating from hydrogen reaction with graphitic-like carbon has been reported to require much higher temperatures (>890°C).[39] Based on the quantification results, the reference K/Mo_2C catalyst exhibits the highest CH_4 desorption, followed by Ni/K/Mo_2C, Cu/K/Mo_2C and Mn/K/Mo_2C. Taking into account both CO and CH_4 desorption, the loss of the catalyst carbon is in the range of 30-45% depending on the catalyst. It should be noted however that neither CO nor CH_4 are formed at temperatures close to those of the CO hydrogenation reaction (250-280°C). Therefore, this catalyst loss is very unlikely to occur during reaction conditions.

Leary et al.[36] also studied the mechanism by which the incorporated oxygen from Mo_2C catalyst is removed during TPR and TPD. In agreement with our results, they concluded that oxygen cannot be removed without also removing a significant amount of bulk carbon and stated that the major difference between the TPD and TPR spectra was the mechanism by which oxygen was removed. In TPD, oxygen was removed by reaction with carbon, whereas in TPR most of the oxygen reacted with hydrogen resulting in high water desorption. However, approximately 15% of the oxygen still reacted with carbon in the sample in line with our results.

Summarizing, the TPD-He and TPR-H_2 results both point out that significant oxygen is incorporated in the molybdenum carbide structure, which could originate from the passivation treatment of the samples and/or their exposure to air, as well as the formation of surface oxidic phases. In order to remove this oxygen that could potentially act as poison to the catalytic reaction and reduce the catalyst, it is thus necessary to pre-treat the samples in-situ prior to reaction with hydrogen at high temperatures. Since in the presence of hydrogen, most oxygen is removed at temperatures up to 500°C, without losing a significant amount of carbon from the catalyst, we selected to pre-treat our samples in pure hydrogen at 500°C for 2h.

In order to study the interaction between Mo and the transition metals in the M-promoted K/Mo_2C catalysts, the surface chemistry and the electronic environment of the metals on the surface was investigated by XPS. The C 1s spectra of all carbide catalysts (Fig. 4 (a)), primarily show two peaks. The peak at 284.8 eV is attributed to graphitic-like carbon,[40] and the peak at 283.7 eV is ascribed to carbidic carbon in the Mo_2C structure. [16, 41] The graphitic-like carbon is probably deposited on the catalytic surface during the carburization synthesis, as reported also by several authors.[16, 41, 50, 66] It is notable that the intensity of the peak at 284.8 eV increases dramatically when the Ni promoter is introduced to K/Mo_2C, indicating a preferential deposition of carbon on Ni/K/Mo_2C. This is confirmed also by the very low exposure of Ni on the surface, as shown in Table 2 and discussed later in the paper. Two smaller peaks located at 286.1 and 288 eV can be attributed to carbon atoms involved in C-O and C=O species due to contamination.[41]

Figure 4 (b) illustrates the Mo 3d XPS spectra of all materials after deconvolution. Charging effects were corrected by referencing the binding energies to the C 1s graphitic carbon peak at 284.8 eV.[40] Characterization with XPS reveals the complexity of the catalysts, as Mo was detected in several oxidation states over all catalysts, ranging from Mo^{6+} to $Mo^{\delta+}$ ($1<\delta<4$). The distribution (shown in Table 2) however differed significantly depending on the nature of the promoter. The reference K/Mo_2C catalyst presents two main peaks at 231.9eV and 228.6eV that can be attributed to the $3d_{3/2}$ and $3d_{5/2}$ transitions of $Mo^{\delta+}$ ($1<\delta<4$). [40, 42] The peak at 227.9 – 228.6 eV has been assigned to the molybdenum atoms in the carbidic phase.[40, 42-44] According to studies by Bao et al., [45] the $Mo^{\delta+}$ species are regarded as the adsorption sites for non-dissociative CO and responsible for alcohol formation. A similar result was obtained by Li et al.,[46] who suggested that the Mo species with intermediate-valence state (averaged around +3.5) are more likely to be the active site for alcohol synthesis from CO hydrogenation. The main second species detected in K/Mo_2C is Mo^{4+} with $3d_{3/2}$ and $3d_{5/2}$ transitions at 232.4 eV and 229.3 eV respectively.[47, 48] Very small concentrations of Mo^{5+} and Mo^{6+} with $3d_{5/2}$ binding energies of 230.5 eV[49] and 232.7 eV[42] were also evidenced on the surface. The presence of Mo at higher oxidation state can be attributed to the passivation of the catalyst prior to exposure in air which leads to the partial and/or total oxidation of some surface molybdenum species. [43, 50] It should be reminded here that no formation of bulk MoO_2 or MoO_3 was evidenced by XRD.

The introduction of the promoters induced significant changes in the oxidation state of Mo on the surface. In all samples, the promoters increased the signals attributed to Mo species with a valence higher than 4. As demonstrated in Table 2, the introduction of nickel led mainly to an increase in the surface Mo^{5+} oxidized species, while in the presence of both Cu and Mn a significant amount of Mo^{6+} is also present on the catalytic surface. Under reaction conditions however, we expect that the concentration of these high oxidation state molybdenum species is low due to the pre-reduction of the catalysts in hydrogen prior to the catalytic measurements. Focusing our attention on the $Mo^{\delta+}$ peak assigned to molybdenum in the carbidic phase, it can be observed that all transition metals induce a shift of the Mo 3d transition to lower binding energies. The effect is stronger in the case of Ni and Mn promotion. This shift signifies strong interaction between the carbide and the dopants and transfer of electrons from Ni and Mn to Mo, leading to an increase in the electron density of molybdenum.[26, 47] Łaniecki et al.[51] also reported that the presence of transition metals enhances the reducibility of Mo species. The increase in the electron density of Mo has important implications on its catalytic performance as discussed later in the paper.

Figure 5 (a), (b) and (c) shows the deconvoluted XPS spectra of the transition metal promoters in the K/Mo_2C catalysts. In the

Ni/K/Mo_2C sample, the Ni 2p spectrum is centred on 853 eV. The binding energy of Ni^0 $2p_{3/2}$ has been reported at 852.6 eV.[52] The shift to slightly higher binding energy in the Ni/K/Mo_2C catalyst can be attributed to the donation of electrons from Ni to Mo (as evidenced also from the shift in the Mo 3d binding energy) and/or electronic interactions with the alkali promoter.[53] These confirm the strong interaction of Ni and Mo in the promoted catalyst and point out to the possible formation of the mixed Ni-Mo carbide phase detected in the XRD pattern of the material. The peak at 856.2 eV with the shakeup satellite at 860.8 eV can be attributed to Ni^{2+} $2p_{3/2}$, characteristic of NiO.[54, 55] The presence of oxidized nickel is probably due to the passivation step of the catalyst prior to air exposure and the formation of a thin NiO film on the surface which we expect that is removed during the catalyst pre-reduction step.

In the Cu/K/Mo_2C catalyst, the chemical valence of Cu on the catalyst surface is a mixture of +1 and +2 valence states, as shown by the peaks at ~ 932.5 eV and 934.8 eV assigned to Cu^{1+} $2p_{3/2}$ and Cu^{2+} $2p_{3/2}$ respectively and the divalent Cu satellite peaks in the 940-945 eV range (see Figure 5b).[56] No metallic copper was detected on the surface, probably due to the easy oxidation of Cu during the catalyst passivation step. Regarding manganese, the Mn $2p_{3/2}$ peaks are in general rather broad and the binding energy shifts are not large enough to clearly distinguish between the different Mn valence states, especially in the case that multiple valences are present.[57] The Mn 2p XPS spectra shown in Fig. 5c presents a broad peak centred on 641.9 eV, which has been attributed to the Mn $2p_{3/2}$ transition of either Mn^{4+} (641.9 eV), Mn^{3+} (641.7 eV) or Mn^{2+} (641.9ev).[58, 59] The presence of the intense satellite structure at 647 eV is however characteristic of MnO species,[60] indicating that the transition at 641.9 eV can be probably assigned to Mn^{2+} species, without excluding the presence of manganese in other oxidation states.

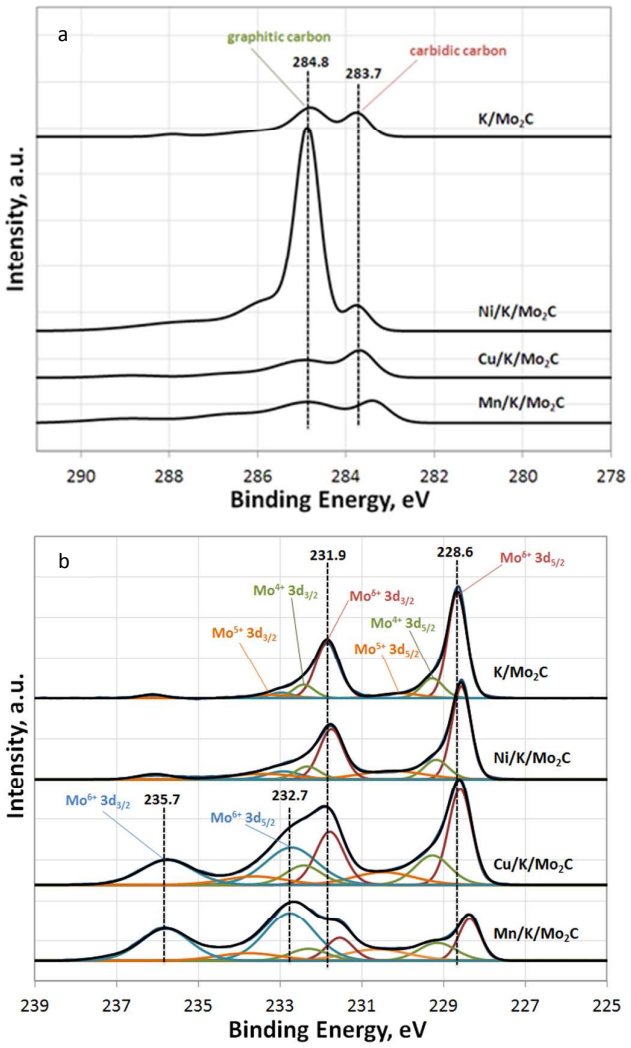

Figure 4. C 1s (a) and Mo 3d (b) XPS spectra of the transition metal promoted M/K/Mo_2C catalysts, where M=Ni, Cu, Mn

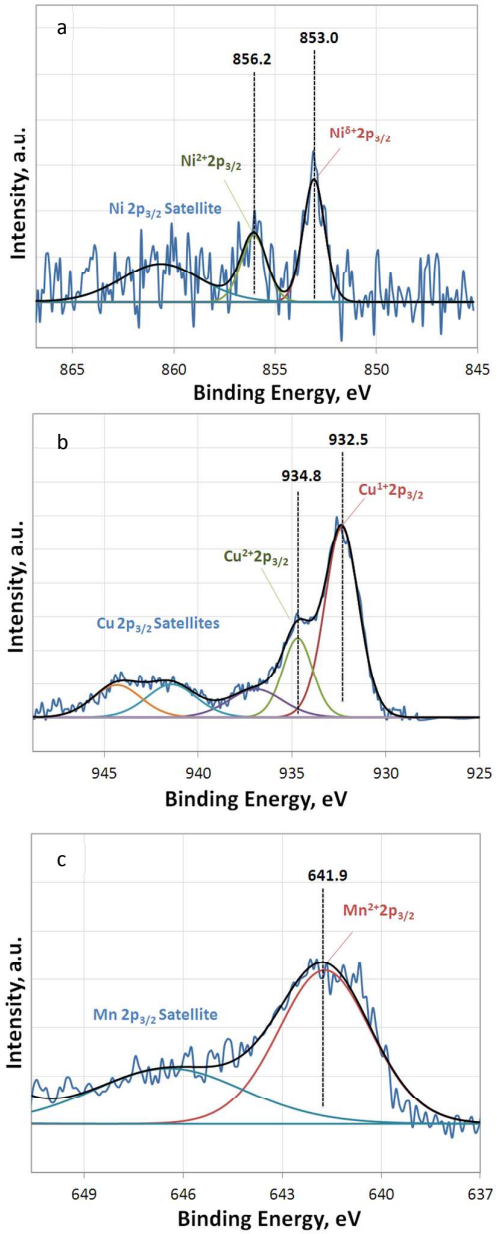

Figure 5. Ni 2p (a), Cu 2p (b) and Mn 2p (c) XPS spectra of the transition metal promoted M/K/Mo_2C catalysts, where M=Ni, Cu, Mn

Table 2. Distribution of Mo species and surface composition of transition metal promoted M/K/Mo2C where M=Ni, Cu, Mn

Catalysts	Mo				Surface ratios		Bulk ratios	
	$Mo^{δ+}$	Mo^{4+}	Mo^{5+}	Mo^{6+}	K/Mo	M/Mo	K/Mo	M/Mo
K/Mo_2C	72.7	15.5	7.2	4.6	0.03	-	0.12	-
Ni/K/Mo_2C	57.5	15.6	17.9	9	0.02	0.04	0.12	0.08
Cu/K/Mo_2C	37.7	17.3	12.8	32.2	0.07	0.16	0.12	0.08
Mn/K/Mo_2C	19.7	14.4	15.4	50.5	0.11	0.15	0.12	0.07

XPS analysis of the passivated carbides was also used to determine the surface composition of the catalysts. Table 2 presents the surface K/Mo and M/Mo (where M is Ni, Cu or Mn) mass ratios in relation to the bulk ratios. For the K/Mo_2C and the Ni-promoted K/Mo_2C, the surface K/Mo ratios are significantly lower than the bulk ones, indicating a poor dispersion of K on the surface. In the carbides promoted with Cu and Mn these values are close to the bulk ones. Concerning the exposure of the promoters, a strong enrichment of the surface in Cu and Mn was detected for Cu/K/Mo_2C and Mn/K/Mo_2C respectively. On the contrary, in the case of Ni, surface exposure is almost half than nominal, designating that at least part of Ni is incorporated in the Mo_2C crystal structure. In combination with the XRD results and the XPS binding energy shifts that point out to the presence of a mixed Ni-Mo phase, it can be inferred that there is strong interaction between Ni and Mo_2C leading to the formation of a mixed Ni-Mo carbidic phase. Xiang et al.[16] also observed, on a similar K/Ni/Mo_2C catalyst, reduction of the Ni/Mo ratio from 1.8 in the bulk to 0.05 on the surface, attributed to incorporation of Ni in the Mo_2C crystal structure and strong Ni-Mo interaction. Another reason for the significantly lower nickel exposure on the surface could be the deposition of graphitic-like carbon formed during carburization preferentially on Ni, as it is well-known that carbon deposits readily on metallic nickel sites. This is supported by the C 1s spectra, presented in Fig 4(a), that show that the peak corresponding to graphitic carbon is much larger in Ni/K/Mo_2C compared to the other catalysts.

Catalytic performance in CO hydrogenation to higher alcohols

The CO hydrogenation experiments were performed over all investigated catalysts at two temperatures (250°C and 280°C) at constant pressure 40 bar and two pressures (40 bar and 60 bar) at constant temperature 280°C to study the reactivity in CO activation and product distribution. The main reaction products attained were C_1-C_6 alcohols (with significant amounts of C_{2+} alcohols), dimethyl ether (DME), C_1-C_6 hydrocarbons, as well as large amount of CO_2 produced via the water gas shift side-reaction. The conversion of CO, the carbon based selectivity to the different products on a CO_2-free basis, the CO_2 selectivity and the yield to total oxygenates (methanol, higher alcohols and DME) are tabulated in Table 3. In this section, we first describe the reaction performance under different operating conditions and then focus on the effect of the specific promoters on the catalytic behavior and the stability of the optimum catalyst.

Table 3. Catalytic performance of the carbide catalysts of transition metal promoted M/K/Mo2C where M=Ni, Cu, Mn (reaction conditions: W/F=0.63 g.s/cm3, H2/CO=2)

Catalysts	Reaction Conditions		CO conversion, %	Total Oxygenates STY, mg/g_{cat}/h	Carbon-based selectivity (CO_2 free), C mol%				CO_2 selectivity, C mol%
	Temperature, °C	Pressure, bar			MeOH	C_{2+}OH	DME	HC	
K/Mo_2C	250	40	1.2	12.9	13.6	59.0	15.5	11.9	30.8
	280	40	5.7	33.9	6.7	15.9	34.2	43.2	43.4
	280	60	5.8	45.2	15.0	29.0	25.5	30.5	40.8
$Ni/K/Mo_2C$	250	40	3.7	24.5	7.8	34.8	27.4	30.0	47.6
	280	40	16.9	94.3	5.5	26.2	24.7	43.6	45.9
	280	60	23.2	147.4	6.4	30.5	23.5	39.6	42.4
$Cu/K/Mo_2C$	250	40	1.8	19.0	6.0	69.2	9.7	15.1	25.7
	280	40	7.3	35.4	6.7	24.2	13.7	55.4	42.7
	280	60	7.4	52.2	13.3	29.4	25.4	31.9	45.5
$Mn/K/Mo_2C$	250	40	1.7	17.3	10.0	64.8	13.8	11.4	32.7
	280	40	5.6	30.4	8.3	25.1	27.2	39.5	51.0
	280	60	5.9	33.7	7.3	30.2	29.7	32.8	52.5

Reaction performance. All carbides exhibited very low activity in CO hydrogenation at 250°C under the current experimental conditions, with conversions ranging from ~1-4%. Increasing the temperature from 250 to 280°C led to CO conversion increase of about 5x on the reference K/Mo_2C catalyst and 4x on all transition metal promoted catalysts, with maximum attained conversion of 17% over $Ni/K/Mo_2C$. In terms of selectivity, the increase of temperature (and conversion) sharply increased the concentration of hydrocarbons, DME and CO_2 at the expense of higher alcohols and methanol formation, in the majority of the catalysts. Higher temperatures, therefore, significantly enhance the formation of hydrocarbons and CO_2 via the water gas shift reaction, in agreement with our previous results regarding higher alcohols formation over bimetallic Ni-Mo catalysts supported on activated carbon[23] and Cu-based catalysts.[31] The increase in hydrocarbons can be related to the higher activation energy for hydrogenation than for CO insertion in the carbonaceous intermediate.[46] Moreover, the increased CO_2 concentration at higher temperatures changes also the H_2/CO ratio in the reactor, indirectly affecting higher alcohol formation.[27, 61, 62]

The effect of increasing pressure from 40 bar to 60 bar at 280°C on reactivity was less pronounced than the temperature effect. For the reference and Cu and Mn-promoted K/Mo_2C catalysts only a minor increase of CO conversion was recorded. Over the $Ni/K/Mo_2C$ sample, the pressure increase improved conversion notably, from 17% to 23%. Regarding the product selectivity, higher pressures led to higher alcohol selectivity at the expense of hydrocarbon formation over all materials, whereas selectivity to CO_2 remained practically unaffected by pressure. This is in line with thermodynamics, according to which higher alcohol synthesis is favored at higher pressures.[61] The production of hydrocarbons has been shown to increase less than higher alcohols with increasing pressure.[64]

Figure 6 illustrates a detailed distribution of the products over $Ni/K/Mo_2C$ at 40 and 60 bar at 280°C. In general, it can be observed that the synthesis yields preferentially DME, low molecular weight hydrocarbons (mainly methane) and linear alcohols with up to five carbon atoms, with small amounts of branched alcohols. According to a review by Surisetty et al.,[65] the alcohol products over alkali-promoted molybdenum-based catalysts are linear alcohols and the mechanism for formation of higher alcohols is via a classical insertion of CO into a CH_x precursor.[7] The presence however of secondary alcohols in the product mix suggests that chain-growth also takes place via an aldol condensation pathway. Evidence of the occurrence of alcohol coupling reactions over sulfided Mo-based catalysts has also been reported by Christensen et al.[27] The high selectivity to methane (~20%) can be ascribed to the methanation activity of Ni, as was also reported by Li et al.[26] Concerning the nature of the produced alcohols, nickel strongly promotes the formation of ethanol, followed by propanol, methanol, butanol and pentanol. The increase in pressure does not significantly alter the distribution to the different alcohols.

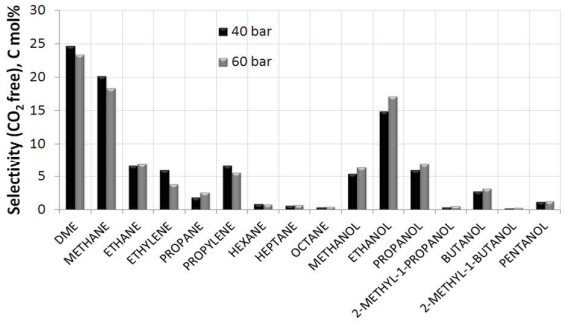

Figure 6. Detailed product distribution over the $Ni/K/Mo_2C$ catalyst at 40 and 60bar (reaction conditions: T=280°C, W/F=0.63 g·s/cm^3, H_2/CO=2)

Effect of promoters. Based on the data in Table 3, it can be observed that promotion with transition metals generally enhanced reactivity towards CO compared to the reference K/Mo_2C. The addition of nickel undoubtedly had the most favorable influence in reactivity, with a maximum attained conversion of 17% at 280°C and 40bar. Cu only slightly improved activity, increasing conversion to ~7.5% from 5.7% for the K/Mo_2C carbide, while Mn demonstrated no activity effect. Similar results under mild pressure conditions as the ones employed in the present study have been reported also by others,[27, 66] although many controversial data appear in literature for the activity of such catalysts under various reaction conditions.[7, 47, 50] The beneficial effect of nickel on activity has been reported by several other researchers,[14, 47, 50] who ascribed it to the excellent methanation ability of Ni. As discussed above, Ni is known to provide very active sites for dissociative chemisorption of CO and subsequent hydrogenation of the CH_x species to methane.

The effect of the dopants on the selectivity to the different products is presented in Figure 7 with data obtained at 280°C and 40bar. At these conditions, the conversion level for all catalysts is similar (~ 5-7%), with the exception of $Ni/K/Mo_2C$ which exhibited higher conversion. All promoters almost doubled selectivity to alcohols higher than methanol compared to the reference catalyst, suggesting that the synergy between Mo and transition metals favours oxygenate formation and carbon chain growth. The effect of Ni and Mn on selectivity is similar, with respect to the fact that this increased higher alcohols concentration originates from suppression of DME formation, while selectivity to methanol and hydrocarbons remains largely unchanged. On the contrary, the Cu promoter although also favours higher alcohol formation, it also further promotes the production of hydrocarbons in expense to DME. Concerning the CO_2 selectivity, it is rather high and ranges between 43-50% over all catalysts, indicating that the transition metal doped Mo_2C catalysts are quite active in the water gas shift reaction. The nature of the promoter does not seem to greatly affect activity towards WGS.

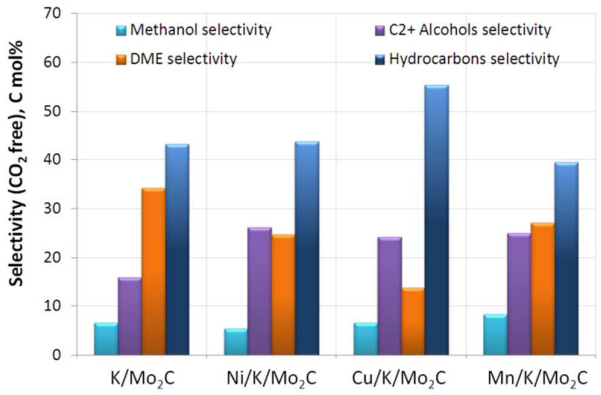

Figure 7. Selectivity (CO_2-free) to the different reaction products over the transition metal promoted $M/K/Mo_2C$ catalysts, where M=Ni, Cu, Mn (reaction conditions: T=280°C, P=40bar, W/F=0.63 g·s/cm^3, $H_2/CO=2$)

Not only the total amount of C_{2+} alcohols, but also the detailed alcohol distribution, is crucial for the suitability of the CO hydrogenation product for fuel applications. Figure 8 illustrates the distribution of produced alcohols over the four investigated molybdenum carbide catalysts at 280°C and 40bar. It can be observed that in contrast to copper-based catalysts where methanol is the main alcohol product with over 80% selectivity,[31] alcohols with carbon number from two to four are the main products over MoC_2 in agreement with literature.[7, 25, 50] Over the reference K/Mo_2C catalyst, ethanol is the most abundant alcohol, followed by descending amounts of methanol, propanol and $C_{4+}OH$. The carbon chain growth pattern for alcohols is influenced by the nature of the promoter, with all promoters reducing the concentration of methanol in the alcohol product. The most pronounced effect is that of nickel, which significantly enhances the formation of ethanol, with equimolar formation of C_1, C_3 and C_4 alcohols. The positive effect of Ni on C_{2+} alcohol selectivity, mainly towards ethanol and propanol, has also been reported in CO hydrogenation over transition metal promoted alkali-doped molybdenum sulfide catalysts.[26] Sun and his group[67] investigated the promotion of $Cu/Mn/ZrO_2$ with Fe, Co and Ni and found that Fischer–Tropsch elements promote carbon chain growth in CO hydrogenation. The presence of nickel in K/MoS_2 catalyst was also found to greatly enhance the C1-C2 homologation step, leading to formation of ethanol as the dominant product.[29]

Mn and Cu on the other hand also promote selectivity to higher alcohols, but in particular to alcohols with 3 and 4+ carbon atoms. This effect is more pronounced with Cu, as the $Cu/K/Mo_2C$ catalyst produces the highest concentration of propanol, butanol and pentanol compared to limited production of methanol and ethanol. In agreement with our results, Christensen et al.[27] reported similar catalytic performance regarding the CO hydrogenation reaction over Cu promoted K/Mo_2C catalysts, claiming that copper particles may contribute to the formation of methanol, which can act as a precursor in the formation of higher alcohols. They also supported that Cu possibly enhances hydrogen transfer reactions.

Summarizing, it appears that all transition metals investigated in this study favour CO hydrogenation to higher alcohols by either increasing CO conversion and/or selectivity to higher alcohols. The most beneficial effects are realized by nickel which not only significantly increases reactivity to carbon monoxide, but it also maintains high preferential formation of higher alcohols, and especially ethanol. Highest performance was attained at 280°C and 60 bar, with ~24% CO conversion and carbon-based selectivity to C_{2+} alcohols over 30%. At these conditions, the $Ni/K/Mo_2C$ catalyst exhibits the highest space time yield to oxygenates, equal to 147.4 mg/g_{cat}·h.

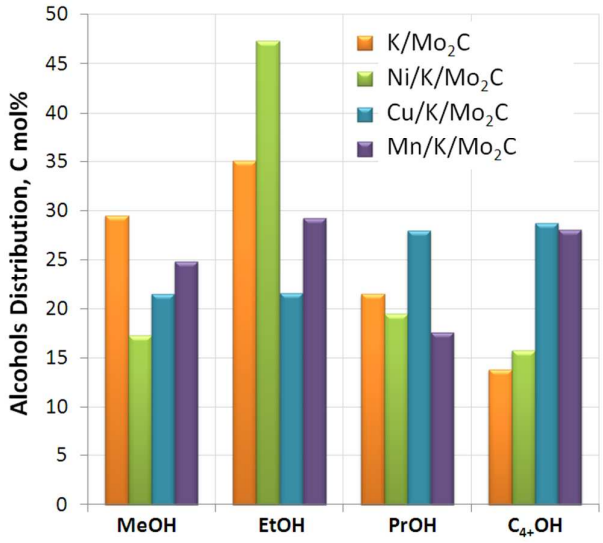

Figure 8. Distribution of alcohols over the transition metal promoted M/K/Mo_2C catalysts, where M=Ni, Cu, Mn, at 280°C (reaction conditions: P=40bar, W/F=0.63 g s/cm^3, H_2/CO=2)

Stability testing of Ni/K/Mo_2C. A long term testing of the optimum catalyst, Ni/K/Mo_2C, was performed in order to examine catalyst stability under the best reaction conditions regarding activity and higher alcohols selectivity. The Ni-promoted K/Mo_2C catalyst was therefore tested at 280°C and 60 bar for a total of 400h time-on-stream and the results are illustrated in Figure 9. The catalyst exhibited a constant, slow deactivation during the first 150 hours on stream, with activity dropping by about ~25%. The catalytic activity continued to decline, albeit with lower deactivation rate, leading to additional 23% loss in conversion after 400 hours of continuous operation. Selectivity did not vary significantly with time-on-stream. A small increasing trend in HAS formation observed with time-on-stream is probably related to the decrease in CO conversion.

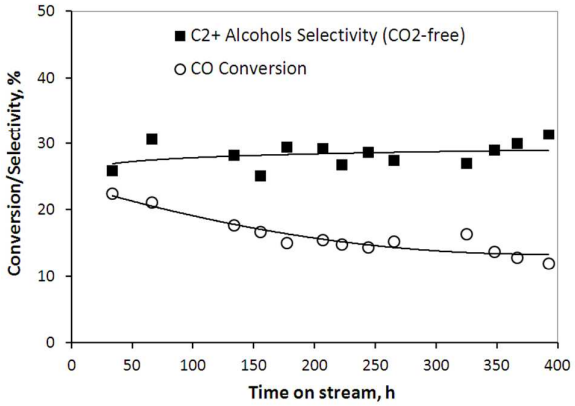

Figure 9. CO conversion and C_{2+} alcohol CO_2-free selectivity with time on stream for the Ni/K/Mo_2C catalyst (reaction conditions: T=280°C, P=60bar, W/F=0.63 g s/cm^3, H_2/CO=2)

In order to elucidate the origin of deactivation, the used catalyst was characterized with BET, XRD, TEM and CHN analysis after the reaction. The specific surface area of the Ni/K/Mo_2C catalyst after the long term experiment was found to be < 0.3 m^2/g, much lower than the initial surface area of 17 m^2/g. The XRD results shown in Figure 10, demonstrate no significant alteration of the Mo_2C crystal phase. However, the exposure of the catalyst to reaction conditions for prolonged periods led to the disappearance of the K_2MoO_4 and Ni-Mo mixed carbidic phases and the formation of a well-defined $K_2Mo_2O_7$ phase and $Ni_2O_2(OH)$. The detection of the hydrated oxidic nickel species points out to a segregation of the Ni-Mo carbide that could be responsible for the observed decrease in CO conversion with time-on-stream. This result was further confirmed by examining the catalyst surface with transition electron microscopy (TEM). Figure 11 illustrates TEM image of the fresh (a) and used Ni/K/Mo_2C catalyst (b, c and d) after the long term experiment. As shown in Fig. 11 (a), the fresh catalyst consists of well crystallized agglomerated carbidic particles, surrounded by a thin film of crystallized carbon, which is more likely ascribed to the carbon of the carbide. The TEM images of the used catalyst are dominated by coke formation. EDS analysis on two distinct particles of the used catalyst, shown in Fig. 11 (b) and 11 (c), revealed the formation of Ni-rich areas (particle I) with Ni content higher than the nominal and Ni-poor particles (particle II), supporting the notion of Ni-Mo carbide segregation. Concerning coke formation, TEM images show that practically all catalyst particles are encapsulated in carbon formations. Fig. 11 (c) for example illustrates well-crystallized agglomerated particles surrounded by amorphous carbon. Due to the carbidic nature of the catalyst, the amount of coke on the used catalyst was determined by difference by measuring the C content of the fresh and used sample. The CHN analysis of the fresh K/Ni/Mo_2C catalyst gave a C content of 11.1 wt%, a value much higher that the nominal 5 wt% C content of the sample. This demonstrates, in accordance with the XPS C 1s results, the formation of a significant amount of graphitic-like carbon during carburization. The C concentration in the used catalyst was measured equal to 38.3 wt%, pointing out to a ~ 27 wt% coke deposition on the surface during the stability test. The great decrease recorded in the surface area after the stability test could be thus ascribed to notable blockage of the catalyst pores by carbon and agglomeration of the catalyst particles. The deposition of coke on the surface obviously contributes also to the deactivation observed with time on stream. The decline in activity due to carbon formation has been widely reported as typical deactivation reason over molybdenum carbide catalysts.[7, 27, 68] Finally, Fig. 11 (d) shows the presence of crystallized carbon, which is more likely ascribed to the carbon of the carbide, since XRD results showed that the Mo_2C crystal phase is retained after the long term experiment.

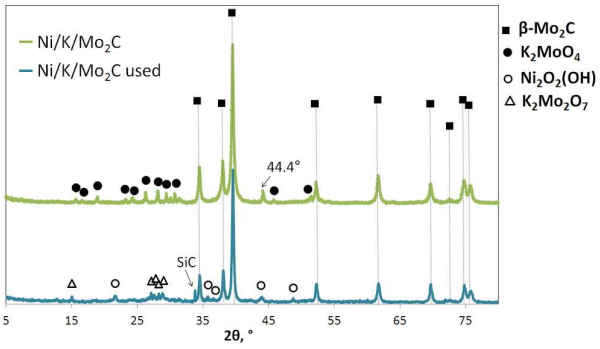

Figure 10. X-ray diffraction patterns of the Ni/K/Mo_2C catalyst, fresh and used after 400 hours of continuous operation

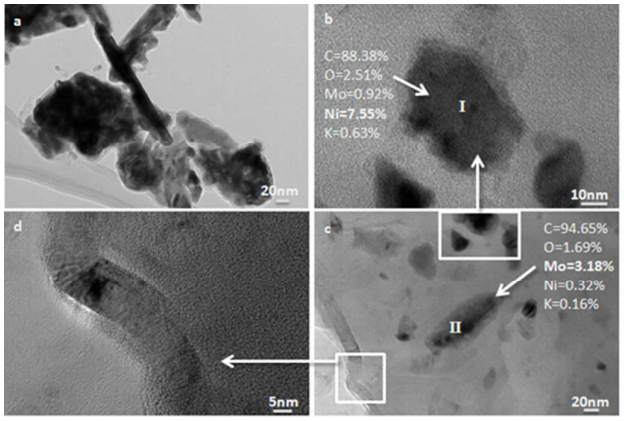

Figure 11. TEM images of the fresh (a) and used (b, c, d) Ni/K/Mo_2C catalyst after 400 hours of continuous operation: (b) Ni-rich area, (c) Ni-Mo carbide segregation due to carbon formation, (d) crystallized carbon area

Discussion

The results presented above confirm, in agreement with previous studies,[14, 25, 27] that alkali-containing Mo_2C catalysts constitute a promising class of catalysts for the hydrogenation of CO to higher alcohols, exhibiting selectivity higher than 20% at mild reaction conditions (low temperature and pressure). The promotion of K/Mo_2C with Ni, Cu and Mn modified both the physicochemical characteristics and the catalytic performance of the carbides. The addition of nickel had the most pronounced effect on activity, where a great increase in CO conversion was recorded. In terms of selectivity, all promoters increased selectivity to higher alcohols, preferentially to ethanol on Ni/K/Mo_2C and to propanol and butanol on Mn- and Cu- promoted carbides.

In general, the formation of higher alcohols from syngas requires a catalyst able to adsorb CO both molecularly and dissociatively. Non-dissociative CO adsorption leads to CH_3OH formation, while dissociative CO chemisorption leads to formation of surface carbon species that are hydrogenated to CH_x intermediates and eventually to hydrocarbons. The existence of both types of sites on the catalytic surface leads to higher alcohol formation via insertion of the non-dissociated CO to the CH_x intermediates. DFT studies on Mo_2C showed that direct CO dissociation is kinetically favorable on the Mo-terminated β-Mo_2C (0001).[24] Pistonesi et al., who studied the effect of K on the adsorption and dissociation of CO on the β-Mo_2C (001) surface by density functional theory calculations, suggested that the activation energy barrier for CO dissociation increases in the presence of potassium.[69] According to the above, the shift of the product distribution from hydrocarbons to alcohols in Mo_2C promoted with alkalis[16] can be attributed to the balanced presence of sites for both CO adsorption and dissociation on the catalytic surface.

The reference K/Mo_2C catalyst in our study mainly produces hydrocarbons indicating that CO dissociative adsorption is the main mechanism of CO activation on the surface. The increase of higher alcohol selectivity over all transition metal promoted catalysts suggests that the dopants modify the electronic properties and provide sites for non-dissociative CO adsorption on the surface. The XPS characterization data showed a clear shift of the Mo 3d transition of molybdenum in promoted Mo_2C to lower binding energies, signifying transfer of electrons from the transition metals to Mo. In analogy to what has been reported for the effect of alkali promoters[69] - that also act as electron donors - on Mo_2C surfaces, it can be suggested that the transition metals increase the activation energy barrier for CO dissociation, thus promoting its molecular adsorption on the surface and the formation of oxygenates.

Most beneficial promotion was achieved by nickel which not only significantly increased reactivity to carbon monoxide, but also promoted ethanol formation, in contrast to the expected increase in hydrocarbons as nickel is known to act as a centre for the dissociative chemisorption of CO. Nagai et al. and Zhu et al. reported that the electronic donation from Ni to Mo atoms results in the increase of d-orbital occupation of molybdenum.[33, 70] According to several studies,[23, 25] the synergy between Ni and Mo promotes alcohol formation through the strong interaction between the two metals. Both the XRD and the XPS results prove this interaction and suggest the formation of a mixed Ni-Mo carbidic phase, possibly Ni_6Mo_6C. Moreover, the composition of the surface measured by XPS shows that Ni is not directly exposed on the surface, as opposed to Cu and Mn in Cu/K/Mo_2C and Mn/K/Mo_2C respectively, thus preventing direct interaction of CO molecules with metallic nickel. Phases such as Ni_6Mo_6C, Co_3Mo_3C and Ni-Mo-S have been suggested to be responsible for the high activity of higher alcohol synthesis in similar catalysts.[16, 71, 72] Similar results for CO adsorption on Co-Mo carbides were also reported by Nagai and Matsuda.[73] Nagai et al.[33] reported that carbon-deficient Ni_6Mo_6C crystallites constitute the active sites in NiMo bimetallic carbide catalysts. They suggested that CO adsorbs molecularly rather than dissociatively on the Ni- and C-terminated surface defect sites of the Ni-Mo bimetallic carbide catalysts, leading to oxygenate rather than hydrocarbon formation.

We can thus summarize that promotion of K/Mo_2C with Ni leads to the formation of a mixed Ni-Mo carbidic phase, where Mo has modified electronic properties due to electron

donation from Ni. These reduced Mo sites in close vicinity with Ni serve as active sites for molecular rather than dissociative adsorption of CO and offer a balance of non-dissociated and dissociated CO species on the catalytic surface, leading to enhanced higher alcohol formation.

Experimental

Catalyst preparation

Transition metal promoted M/K/Mo_2C (where M = Ni, Mn, Cu) catalysts, with a constant molar composition of $M_{0.25}K_{0.6}Mo_2C$, were prepared via direct carburization of the $MMoO_x$ oxide precursors. A K/Mo_2C sample with the same K content was also prepared as reference material. The $MMoO_x$ oxide precursors for the bimetallic carbides were prepared by mechanically mixing the appropriate amount of the solid precursors: ammonium heptamolybdate $[(NH_4)_6Mo_7O_{24}\cdot 4H_2O$ (Aldrich)] and the nitrate salt of the corresponding transition metal promoter [$Ni(NO_3)_2\cdot 6H_2O$ (Aldrich), $Cu(NO_3)_2\cdot 3H_2O$ (Merck), $Mn(NO_3)_2\cdot 4H_2O$ (Merck)]. The mixture was then calcined at 500°C under air flow for 6 hours. Carburization was carried out under atmospheric pressure in a flow of 20% CH_4/H_2 gas mixture. The temperature was linearly increased with a rate of 3°C/min from room temperature to 280°C and then to 700°C with a rate of 1°C/min, where it was maintained for 3h. Prior to air exposure, passivation was performed at room temperature in a 3.0 % O_2/He flow. For K addition, the appropriate amount of solid K_2CO_3 (Aldrich) was mechanically mixed with the carburized catalyst. The solids were thoroughly mixed to ensure homogeneity and the final material was calcined at 500°C for 2h under N_2.

Catalyst characterization

For the determination of surface area (BET method) and pore volume, N_2 adsorption/desorption experiments were conducted at −196 °C, using an Automatic Volumetric Sorption Analyzer (Autosorb-1MP, Quantachrome). Prior to the measurements, the samples were dehydrated in vacuum at 250°C overnight.

X-Ray Diffraction (XRD) patterns were obtained using a Siemens D500 diffractometer, employing Cu Kα radiation.

CHN Elemental analysis, in order to determine the carbon content of the carbide catalysts, was carried out on a CHN-800 elemental analyzer (LECO Corporation, USA) according to the UOP 703 method.

Temperature programmed desorption (TPD) in helium was performed in a home-made gas flow system equipped with a quadrupole mass analyzer (Omnistar, Balzers). Typically, the catalyst sample (200mg) was placed in a quartz reactor. The temperature was then raised from room temperature to 800°C with a heating rate of 10°C/min in He flow (50cm^3/min) and was maintained constant at 800°C for 1h. The main (m/z) fragments registered were: CO_2=44, CO=28, H_2O=18, CH_4=16 and He=4. The reduction characteristics of the catalysts were studied by temperature programmed reduction (TPR). Experiments were performed on the same apparatus as described above. Typically, the catalyst sample (200mg) was placed in a quartz reactor and was pretreated in flowing He for 0.5h at 350°C, followed by cooling at room temperature. The temperature was then raised from room temperature to 800°C with a heating rate of 10°C/min in a 5%H_2/He flow (50cm^3/min) and was maintained constant at 800°C for 1h. The main (m/z) fragments registered were: CO_2=44, CO=28, H_2O=18, CH_4=16, He=4 and H_2=2.

X-ray photoelectron spectroscopy (XPS) was carried out using a Kratos Analytical AXIS ultra DLD spectrometer equipped with a monochromatic Al X-ray source. Binding energy (BE) referencing was employed using the adventitious carbon peak at 284.8eV. XPS spectra were recorded with pass energy of 20eV, a step of 0.1eV and X-ray power of 150W. Deconvolution of the peaks was performed with a Kratos Vision software (Version 2.2.10) using Shirley background subtraction and mixed Gaussian-Lorentzian functions.

Electron microscopy was performed on a JEOL 2011 high resolution transmission electron microscope, operating at 200 kV, with a point resolution of 0.23 nm and Cs = 1.0 mm, fitted with an Oxford Instruments INCAx-sight liquid nitrogen cooled EDS detector with an Si(Li) window for EDS analysis. Processing of the spectra was accomplished using the INCA Microanalysis Suite software.

Catalytic reaction tests

The catalytic performance of the samples in carbon monoxide hydrogenation was evaluated in a high pressure small-scale test unit, equipped with three gas lines controlled by high accuracy mass flow controllers. The unit operates with a stainless steel fixed bed reactor (ID: 9.3mm), externally heated with a three-zone furnace, while the exit stream of the reactor is cooled via a heat exchanger and is directed to a system of vessels for the separation and collection of the liquid and gaseous products. The reaction temperature is monitored with a thermocouple inserted in the catalytic bed. The test facility can operate to a temperature range up to 600°C and pressures up to 100 atm.

The samples were first diluted with equal amount of SiC particles of the same size to achieve isothermal operation and were then loaded in the fixed bed reactor. The catalysts were pre-reduced in situ in pure hydrogen at 500°C for 2h and atmospheric pressure. The reacting mixture (CO and H2) was then introduced in the reactor and temperature and pressure were fixed to the desired levels. The higher alcohol synthesis reaction was investigated under the following standard reaction conditions: temperature 280°C, pressure 40 bar, W/F ratio of 0.63 g.s/cm3 and inlet feed composition H2/CO=2. The effect of temperature was studied in the range of 250 to 280°C and the effect of pressure in the range of 40 to 60bar. The steady-state activity measurements were taken after at least 24 h on-stream. The gaseous products were analyzed on-line, while liquids were collected in a trap (-15°C) for 24h and were analyzed offline. The analysis was performed with a GC Agilent 7890A equipped with two detectors (FID & TCD) and three

columns (MS, Porapak Q and DB-FFAP) in a series-bypass configuration.

CO conversion was calculated as the percentage of carbon monoxide converted to products:

$$\text{CO conversion (mol\%)} = \frac{\text{moles of CO}_{in} - \text{moles of CO}_{out}}{\text{moles of CO}_{in}} \times 100 \quad (1)$$

Carbon selectivity was defined as the moles of carbon in a given product to the total moles of converted carbon:

$$\text{Selectivity (C mol\%)} = \frac{\text{moles of a given product} \times \text{number of carbons in product}}{CO_{in} - CO_{out}} \quad (2)$$

Space time yield (STY) was calculated as the weight of each oxygenated compound produced per unit mass catalyst and per time unit:

$$\text{STY (mg/g}_{cat}\text{.h)} = \frac{\text{weight of oxygenated compound}}{\text{catalyst weight} \times \text{time}} \quad (3)$$

Conclusions

Potassium containing molybdenum carbides doped with Ni, Cu and Mn were found to be promising catalysts for the hydrogenation of CO to higher alcohols. The main reaction products over the investigated materials were linear alcohols with two to five carbon atoms, methanol, low molecular weight hydrocarbons and DME. All the transition metals exerted a promotional effect on the selectivity to higher alcohols, doubling the selectivity to higher alcohols compared to the reference material at 280°C and 40 bar. In terms of activity, the CO conversion of the catalysts promoted by Cu and Mn was found to be very similar to that of the reference K/Mo_2C catalyst. Nickel on the other hand greatly increased activity, reaching a maximum CO conversion of 23% at 280°C and 60 bar with higher alcohol selectivity equal to 30.5% (mainly ethanol).

Characterization with XRD showed that β-Mo_2C is the main crystal phase in the catalysts. The passivation step and/or exposure to air lead to formation of surface oxidic phases and oxygen incorporation in the carbides. TPR studies showed that this oxygen can be efficiently removed without losing significant amount of carbon during reduction with hydrogen at temperatures lower than 550°C. Investigation of the catalysts by XPS revealed the strong interaction between molybdenum in the carbidic phase and the dopants, as in the presence of the transition metals a significant shift of the Mo 3d binding energy was recorded, indicative of electron transfer to the Mo atoms. The most pronounced interaction was observed in the case of the optimum Ni/K/Mo_2C catalyst, where both XRD and XPS results point out to the formation of a mixed Ni-Mo carbidic phase, probably Ni_6Mo_6C. These sites are likely to be responsible for the enhanced higher alcohol formation, serving as active sites for molecular rather than dissociative adsorption of CO and offering a balance of non-dissociated and dissociated CO species on the catalytic surface.

The stability of the optimum Ni/K/Mo_2C catalyst was tested in a long term test for 400 hours continuous operation at constant conditions. Significant deactivation was observed, with CO conversion decreasing by ~48%. Post-reaction catalyst characterization revealed extensive carbon formation and total loss of the surface area (<0.3m^2/g). Moreover, the exposure of the catalyst to the reaction conditions for prolonged periods led to the disappearance of the mixed Ni-Mo carbidic phase and the formation of a well-defined $K_2Mo_2O_7$ phase and Ni_2O_2(OH). The segregation of Ni_6Mo_6C and the subsequent formation of hydrated oxidic nickel species, together with the extensive deposition of coke on the surface, could be responsible for the observed decrease in CO conversion with time-on-stream.

Acknowledgements

Dr P. Patsalas and Mr N. Pliatsikas from the Physics Department of the Aristotle University of Thessaloniki are gratefully acknowledged for the XPS measurements. These results have been achieved within the framework of the project “European Multilevel Integrated Biorefinery Design for Sustainable Biomass Processing - EuroBioRef”, funded by the EU under the 7th Framework Programme of the European Union for the funding of research and technological development in Europe. The author Eleni Liakakou would like in addition to acknowledge financial support from European Union (European Social Fund - ESF) and Greek national funds through the Operational Program "Education and Lifelong Learning" of the National Strategic Reference Framework (NSRF) - Research Funding Program: THALES. Investing in knowledge society through the European Social Fund.

References

1 Eurobioref Public Booklet, Available from: http://eurobioref.org/images/Eurobioref_livret_resultats_total_v4.pdf (accessed July 2015)
2 V.R. Surisetty, A.K. Dalai, J. Kozinski, *Appl. Catal. A: Gen.* 2011, **404**, 1
3 R.G. Herman, *Catal. Today,* 2000, **55**, 233
4 J.J. Spivey, A. Egbebi, *Chem. Soc. Rev.,* 2007, **36**, 1514
5 V. Subramani, S.K. Gangwal, *Energy Fuels,* 2008, **22,** 814
6 P.M. Patterson, T.K. Das, B.H. Davis, *Appl. Catal. A: Gen.,* 2003, **251**, 449
7 H.C. Woo, K.Y. Park, Y.G. Kim, I-S. Namau, J.S. Chung, J.S. Lee, *Appl. Catal.,* 1991, **75,** 267
8 M. Saito, R.B. Anderson, *J. Catal*., 1980, **63**, 438
9 K.Y. Park, W.K. Seo, J.S. Lee, *Catal. Lett*., 1991, **11**, 349
10 J. Patt, D. Moon, C. Phillips, L. Thompson, *Catal. Lett.,* 2000, **65,** 193
11 S. Ramanathan, S. Oyama, *J. Phys. Chem.* 99 (1995) 16365-16372

12 E.A. Blekkan , C. Pham-Huu , M.J. Ledoux , J. Guille, *Ind. Eng. Chem. Res.,* 1994, **33,** 1657
13 R.B. Anderson, *The Fisher-Tropsh Synthesis*, Academic Press, London, 1984
14 M. Xiang, D. Li, H. Xiao, J. Zhang, H. Qi, W. Li, B. Zhong, Y. Sun, *Fuel,* 2008, **87,** 599
15 M. Xiang, D. Li, H. Xiao, J. Zhang, H. Qi, W. Li, B. Zhong, Y. Sun, *Fuel,* 2006, **85**, 2662
16 M. Xiang, D. Li, W. Li, B. Zhong, Y. Sun, *Catal. Commun.,* 2007, **8**, 513
17 H. Shou, R. Davis, *J. Catal*., 2011, **282,** 83
18 J. Lee, S. Kim, Y. Kim, *Top. Catal*., 1995, **2,** 127-140
19 A. Muramatsu, T. Tatsumi, H. Tominaga, *Bull. Chem. Soc. Jpn*., 1987, **60,** 3157
20 Z-r. Li, Y-l Fu, M. Jian, M. Meng, Y-n Xie, T-d. Hu, T. Liu, *Catal. Lett*., 2000 **65,** 43
21 E. C. Alyea, D. He and J. Wang, *Appl. Catal. A,* 1993 **104**, 77
22 D.B. Li, C. Yang, W.H. Li, Y.H. Sun, B. Zhong, *Top. Catal*., 2005, **32**, 233
23 E.T. Liakakou, E. Heracleous, K.S. Triantafyllides, A.A. Lemonidou, *Appl. Catal. B: Environ.,* 2014 **165,** 296
24 S. Zaman, K. J. Smith, *Cat. Rev. - Sci. Eng*., 2012, **54,** 41
25 L. Zhao, K. Fanga, D. Jianga, D. Li, Y. Sun, *Catal. Today*, 2010, **158,** 490
26 D. Li, C. Yang, H. Qi, H. Zhang, W. Li, Y. Sun, B. Zhong, *Catal. Commun*., 2004, **5,** 605
27 J.M. Christensen, L.D.L. Duchstein, J.B. Wagner, P.A. Jensen, B. Temel, A.D. Jensen, *Ind. Eng. Chem. Res*., 2012, 51, 4161
28 J.-L. Dubois, K. Sayama, H. Arakawa, *Chem. Lett.,* 1992, **21,** 5
29 H.J. Qi, D.B. Li, C. Yang, Y.G. Ma, W.H. Li, Y.H. Sun and B. Zhong, *Catal. Commun.,* 2003, **4**, 339
30 A.B. Stiles, F. Chen, J. B. Harrison, X. Hu, D.A. Storm, H.X. Yang, *Ind. Eng. Chem. Res.,* 1991, **30,** 811
31 E. Heracleous, E.T. Liakakou, A.A. Lappas, A.A. Lemonidou, *Appl. Catal. A*., 2013, **455,** 145
32 Q. Wu, PhD Thesis, Technical University of Denmark, Department of Chemical Engineering, 2013
33 M. Nagai, A.Md. Zahidul, K. Matsuda, *Appl. Catal. A: Gen*., 2006, **313,** 137
34 A.M. Stux, C. Laberty-Robert, K.E. Swider-Lyons, *J. Solid State Chem*., 2008, **181,** 2741
35 J.M. Newsam, A.J. Jacobson, L.E. McCandlish, R.S. Polizzotti, *J. Solid State Chem.,* 1988, **75**, 296
36 L.J. Leary, J.N. Michaels, A.M. Stacy, *J. Catal*., 1986, **101**, 301
37 Z. Malaibari, E. Croiset, A. Amin, W. Epling, *Appl. Catal. A: Gen.,* 2015, **490**, 80
38 S.K. Bej, C.A. Bennett, L.T. Thompson, *Appl. Catal. A: Gen*., 2003, **250**, 197
39 K. Oshikawa, M. Nagai, S. Omi, *J. Phys. Chem.* B, 2001, **105**, 9124
40 J.-G. Choi, L.T. Thompson, *Appl. Surf. Sci.,* 1996, **93**, 143-149
41 P. Delporte, F. Meunier, C. Phamhuu, P. Vennegues, M.J. Ledoux, J. Guille, Catal. Today 23 (1995) 251
42 M. Zhang, W. Zhang, W. Xie, Z. Qi, G. Wu, M. Lv, S. Sun, J. Bao, *J. Mol. Catal. A: Chem*., 2014, **395**, 269
43 T.P.S. Clair, S.T. Oyama, D.F. Cox, S. Otani, Y. Ishizama, R.-L. Lo, K.-I. Fukui, Y. Iwasawa, *Surf. Sci*., 1999, **426**, 187
44 D.C. Song, J. Li, Q. Cai, *J. Phys. Chem*. C, 2007, **111**, 18970
45 M. Lv, W. Xie, S. Sun, G. Wu, L. Zheng, S. Chu, C. Gao, J. Bao, *Catal. Sci. Technol*., 2015, **5,** 2925
46 X.G. Li, L.J. Feng, L.J. Zhang, D.B. Dadyburjor, E.L. Kugler, *Molecules,* 2003, **8**, 13
47 L. Zhao, K. Fanga, D. Jianga, D. Li, Y. Sun, *Catal. Today*, 2010, **158**, 490
48 N. Wang, K. Fang, D. Jiang, D. Li, Y. Sun, *Catal. Today*, 2010), **158**, 241
49 B.P. Barbero, L.E. Cadús, *Appl. Catal. A: Gen*., 2003, **252**, 133
50 M. Xiang, J. Zou, *Journal of Catalysts,* 2013, Article ID 195920, 5 pages
51 M. Łaniecki, M. Małecka-Grycz, F. Domka, *Appl. Catal. A,* 2000, **196**, 293
52 A.P. Grosvenor, M.C. Biesinger, R.St.C. Smart, N.S. McIntyre, *Surf. Sci*., 2006, **600**, 1771
53 Y. Miyamoto, M. Akiyama, M. Nagai, *Catal. Today*, 2009, **146**, 87
54 B. P. Löchel, H.-H. Strehblow, *J. Electrochem Soc.*, 1984, **131**, 713
55 E. Heracleous, A.F. Lee, K. Wilson, A.A. Lemonidou, *J. Catal*., 2005, **231**, 159
56 J.A. Rodriguez, J.Y. Kim, J.C. Hanson, M. Pérez, A.I. Frenkel, *Catal. Lett*., 2003, **85**, 247
57 V.Di Castro, G. Polzonetti, *J. Electron. Spectrosc. Relat. Phenom*., 1989, **48**, 117
58 H.J. Tan, J. Klabunde, P.M.A. Sherwood, *J. Am. Chem. Soc*., 1991, **113**, 855
59 J.C. Carver, G.K. Schweitzer, T.A. Carlson, *J. Chem. Phys*., 1972, **57**, 973
60 M.A. Langell, C.W. Hutchings, G.A. Carson, M.H. Nassir, *J. Vac. Sci. Technol. A*, 1996, **14**, 1656
61 X. Xiaoding, E. B. M. Doesburg, J.J.F. Scholten, *Catal. Today*, 1987, **2**, 125
62 N. Tien-Thao, H. M. Zahedi-Niaki, H. Alamdari, S. Kaliaguine, *J. Catal*., 2007, **245**, 348
63 X. Xu, E.B.M. Doesburg, J.J.F. Scholten, *Catal. Today*, 1987, **2**, 125
64 P. Forzatti, E. Tronconi, I. Pasquon, *Catal. Rev. Sci. Eng*., 1991, **33**, 109
65 V.R. Surisetty, A.K. Dalai,J. Kozinski, *Appl. Catal. A: Gen*., 2011, **404**, 1
66 A. Griboval-Constant, J.-M. Giraudon, G. Leclercq, L. Leclercq, *Appl. Catal. A,* 2004, **260**, 35
67 L. Zhao, R. Xu, W. Wei, Y. Sun, *React. Kinet. Catal. Lett.*, 2002, **75**, 297
68 X. Dong, X.L. Liang, H.Y. Li, G.D. Lin, P. Zhang, H.B. Zhang, *Catal. Today*, 2009, **147**, 158
69 C. Pistonesi, M.E. Pronsato, L. Bugyi, A. Juan, *J. Phys. Chem. C*, 2012, **116**, 24573
70 Q.L. Zhu, B. Zhang, J. Zhao, S.F. Ji, J. Yang, J.X. Wang, H.Q. Wang, *J. Mol. Catal. A: Chem*, 2004, **213**, 199
71 D.B. Li, C. Yang, H.R. Zhang, W.H. Li, Y.H. Sun, B. Zhong, *Stud. Surf. Sci. Catal.*, 2004, **147**, 391
72 D.B. Li, C. Yang, H.J. Qi, W.H. Li, Y.H. Sun, B. Zhong, *Catal. Commun*., 2003, **5**, 605
73 M. Nagai, K. Matsuda, *J. Catal*., 2006, **238**, 489